HHS Public Access

Author manuscript

ACS Sens. Author manuscript; available in PMC 2026 January 07.

Published in final edited form as:

ACS Sens. 2024 May 24; 9(5): 2356–2363. doi:10.1021/acssensors.3c02382.

Modulating Nonlinear Acoustic Response of Phospholipid-Coated Microbubbles with pH for Ultrasound Imaging

Shariq Ali,
Department of Radiology, University of Texas Southwestern Medical Center, Dallas, Texas 75390-8514, United States

Caroline de Gracia Lux,
Department of Radiology, University of Texas Southwestern Medical Center, Dallas, Texas 75390-8514, United States

Katherine Brown,
Department of Bioengineering, University of Texas at Dallas, Richardson, Texas 75080-3021, United States

Connor Endsley,
Department of Radiology, University of Texas Southwestern Medical Center, Dallas, Texas 75390-8514, United States

Adam Woodward,
Department of Radiology, University of Texas Southwestern Medical Center, Dallas, Texas 75390-8514, United States

Robert Mattrey,
Department of Radiology, University of Texas Southwestern Medical Center, Dallas, Texas 75390-8514, United States

Jacques Lux
Department of Radiology, University of Texas Southwestern Medical Center, Dallas, Texas 75390-8514, United States

Abstract

Activatable microbubble contrast agents for contrast-enhanced ultrasound have a potential role for measuring physiologic and pathologic states in deep tissues, including tumor acidosis. In this study, we describe a novel observation of increased harmonic oscillation of phosphatidylcholine microbubbles (PC-MBs) in response to lower ambient pH using a clinical ultrasound scanner. MB echogenicity and nonlinear echoes were monitored at neutral and acidic pH using B-mode and

Corresponding Author: Jacques Lux – Department of Radiology, University of Texas Southwestern Medical Center, Dallas, Texas 75390-8514, United States; jacques.lux@utsouthwestern.edu.

Author Contributions

SA and JL designed the study. SA performed experiments, analyzed data, and designed the figures. CE and AW performed experiments. CDG, KB, RM, and JL analyzed the data and designed the figures. The manuscript was written through contributions of all authors.

Complete contact information is available at: https://pubs.acs.org/10.1021/acssensors.3c02382

The authors declare no competing financial interest.

Cadence contrast pulse sequencing (CPS), a harmonic imaging technique at 7.0 and 1.5 MHz. A 3-fold increase in harmonic signal intensity was observed when the pH of PC-MB suspensions was decreased from 7.4 to 5.5 to mimic normal and pathophysiological levels that can be encountered *in vivo*. This pH-mediated activation is tunable based on the chemical structure and length of phospholipids composing the MB shell. It is also reliant on the presence of phosphate groups, as the use of lipids without phosphate instead of phospholipids completely abrogated this phenomenon. The increased harmonic signal likely is the result of increased MB oscillation caused by a decrease of the interfacial tension induced at a lower pH, altering the lipid conformation. While relative signal changes are interpreted clinically as mostly related to blood flow, pH effects could be significant contributors, particularly when imaging tumors. While our observation can be used clinically, it requires further research to isolate the effect of pH from other variables. These findings could pave the way toward for the development of new smart ultrasound contrast agents that expand the clinical utility of contrast-enhanced ultrasound.

Graphical Abstract

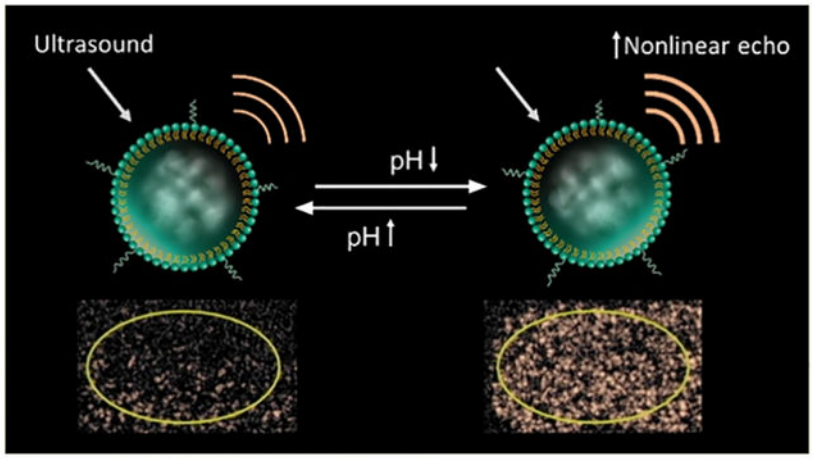

Keywords

Contrast-Enhanced Ultrasound; Microbubble; Phospholipid; pH; Biosensor

The advent of harmonic imaging of microbubbles (MBs) has revolutionized the field of contrast-enhanced ultrasound (CEUS).[1] When tissues are exposed to ultrasound, they produce echoes at the same frequency as the frequency emitted by the ultrasound probe. Since MBs exposed to ultrasound oscillate nonlinearly, they produce echoes containing both the transmit frequency and its harmonics. By filtering the transmit frequency from the received echoes, images will show only MBs with markedly improved contrast resolution.[2] As MBs are restricted to the intravascular space, tissue enhancement can be used to estimate relative tissue blood flow and fractional blood volume.[3] Owing to these features, MBs are routinely used in clinical practice to characterize time-dependent enhancement patterns to recognize tumors from normal tissue, usually liver and kidney.[4] Current MBs consist of a water-insoluble and inert perfluorocarbon gas core stabilized by a shell typically composed of lipids such as phosphatidylcholines (PCs).[5] The combination of the perfluorocarbon

vapor core and stabilizing shell allows MBs to be stable in the vascular space for several minutes despite the slow changes in ambient pressure that occur as they traverse through the circulation, as well as microsecond changes that occur between the compression and rarefaction phases of an ultrasound wave produced by clinical scanners.[6] The type of lipid used allows the shell to buckle during compression or rupture during expansion, which increases the generation of harmonics.[7,8] Comparisons between theoretical simulations and experimental MB dynamic responses corroborate the observation that both MB shell composition and microstructure directly impact MB rheological properties, which are the main drivers of MB dynamic response, including oscillation amplitudes and resonant radii at harmonic and subharmonic resonances. Increasing shell stiffness and viscosity dampens MB oscillation amplitude, while a reduction in interfacial tension at the PFC–water interface that decreases shell viscosity and stiffness increases MB oscillation amplitude.[8–12] Because cross-linking shell lipids decreases or eliminates MB nonlinear response to ultrasound, most likely by restricting MB oscillation, utilizing cross-linkers that are cleavable by chemical, enzymatic, or other stimuli generates harmonics allowing detection of these bioresponsive MBs.[13–15] The successful demonstration of these approaches has paved the way to providing biomarker-responsive ultrasound contrast agents.

In addition to cross-linking, the acoustic response of phospholipid coated MBs can also be modulated by altering shell composition, which affects the acoustic lipid dissolution rate caused by shell lipid shedding and fragmentation. The acoustic response can also be affected by increasing the number of carbons in the phospholipids' acyl chain to increase the attractive intermolecular dispersion force enhancing shell cohesion and greater resistance to ultrasound destruction occurring at both low and high pressure.[16]

In this study, we describe a novel observation that phosphatidylcholine-based MBs (PC-MBs) without cross-linking exhibit pH-dependent harmonic signal (oscillation) changes (Figure 1). Lowering the pH from 7.4 to 5.5 causes a steep increase in the harmonic signal. We also show that this observation is reversible and dependent on the chemical structure of the phospholipids used.

Tissue enhancement on real-time CEUS studies utilizing PC-MBs is directly proportional to MB concentration, and image contrast is caused by relative differences in blood flow and fractional blood volume. With this report, we show that pH also affects image contrast and could therefore potentially be affected by ambient pH during CEUS studies. Though blood pH is tightly controlled in vivo, acidosis is a hallmark of many pathologic states such as ischemia and malignancy due to increased local H^+ concentration and elevated serum lactate.[17,18] For instance, extracellular pH of solid tumors can fall within a range of 6.7–7.1,[19] which is within the range of activation of PC-MBs (Figure 2). As a result, the pH-dependent harmonic signal enhancement from PC-MBs could potentially be exploited to detect the acidic environment of solid tumors—a feature that is associated with increased local aggressiveness, metastatic potential, and chemoresistance.[20] Importantly, this strategy could be readily deployed in the clinic since the FDA approved formulations Lumason and Definity are both PC-MBs.

Methods of mapping tumor pH have been proposed for MRI, PET, photoacoustic, and optical imaging, though none are in routine clinical use.[21,22] Should the effect of pH on PC-MBs be uniquely quantified, ultrasound would hold several advantages over other modalities, including the ability to perform high-resolution real-time imaging of both superficial and deep tissues as well as low cost and widespread clinical availability. Because CEUS is also routinely used for image guided biopsies, sampling acidotic regions would maximize the yield for pathologic analysis. While future work is needed to fully understand the mechanisms behind this observation, our study may serve as the basis for the development of MBs with greater sensitivity to pH and potentially other physiologic and pathologic stimuli.

EXPERIMENTAL SECTION

14:0 PC (1,2-dimyristoyl-*sn*-glycero-3-phosphocholine), 16:0 PC (1,2-dipalmitoyl-*sn*-glycero-3-phosphocholine), 18:0 PC (1,2-distearoyl-*sn*-glycero-3-phosphocholine), 20:0 PC (1,2-diarachidoyl-*sn*-glycero-3-phosphocholine), and 18:0 TAP (1,2-distearoyl-3-trimethylammoniumpropane chloride) were purchased from Avanti Polar Lipids (AL, USA). 18:0 PE-PEG2k (N-(methylpolyoxyethylene oxycarbonyl)-1,2-distearoyl-*sn*-glycero-3-phosphoethanolamine) was purchased from NOF America (NY, USA). Perfluorobutane (PFB) was purchased from FluoroMed (TX, USA). Lumason is distributed by Bracco Diagnostics (NJ, USA) and was collected from the ultrasound clinic shortly after reconstitution. Phosphate-buffered saline, hydrochloric acid, sodium hydroxide, glycerol, propylene glycol, and other chemicals were purchased from ThermoFisher Scientific (MA, USA).

Preparation of PC-MBs.

PC-MBs were prepared as previously described.[23] Briefly, lipid films were prepared by dissolving the desired ratios of lipids in chloroform in glass vials, followed by the removal of chloroform by rotary evaporation (40 °C) to yield thin lipid films. Films were subsequently dried overnight under a vacuum and stored at −20 °C until further use. Lipid films were solvated in a solution of PBS 1X containing propylene glycol and glycerol (80:10:10, v/v/v, 10 mL, final lipid concentration 2 μM) and heated to 70 °C in a bath sonicator (CPX2800H Digital Heated Ultrasonic Cleaner, Branson). Solvated films were then tip sonicated (SFX 550, Model 102-C converter, Branson) with a 1/8 in. tip for 5 s at 70% amplitude (385 W) under a headspace of PFB vapor. MBs were then washed by low-speed centrifugation (300*g*, 3 min) and the infranatant discarded. Washes were repeated 2 times with PBS. The resulting MB suspensions were stored at 4 °C and used within 1 week. MB size distribution and concentration were evaluated before each imaging experiment using a Coulter counter (Multisizer 4, Beckman). Lumason MBs were reconstituted according to package instructions, kept at room temperature, and used within 24 h of reconstitution.

In Vitro Ultrasound Imaging of MBs.

All experiments used 3 mL of PBS prewarmed to 37 °C in a flexible polyethylene transfer pipet bulb containing 1×10^4 MBs/mL. The bulb was placed in a tissue-mimicking phantom

composed of 1% agarose (w/v) and 0.5% cornstarch (w/v) in a 37 °C water bath.[24] Imaging was performed using a clinical ultrasound scanner (Siemens ACUSON Sequoia 512) using either a 15L8 transducer operated at a central transmit frequency of 7.0 MHz at 0.07 mechanical index (MI) or a 4 V1 transducer operated at a transmit frequency of 1.5 MHz at 0.04 MI. MBs were imaged using a dual display standard B-mode and Cadence contrast pulse sequence (CPS) reconstructed from the same data set. CPS transmits 3 consecutive pulses utilizing both amplitude modulation and phase inversion. Brightness mode (grayscale, B-mode) was used for spatial orientation. The focal zone of the transducer was positioned at the far border of the imaging chamber. A prototype Sequoia MSP/MSRQ software installed by Siemens was utilized to acquire frames with real time motion correction that displayed the mean intensity within a region of interest (ROI) for every frame. The ROI was drawn totally within the imaged MB suspension for real-time observation of harmonic intensity (Figure 2). In one set of experiments, MBs were added to PBS, and the pH was adjusted by adding 1 M HCl or 1 M NaOH to reach the desired pH as measured by a pH meter (Mettler Toledo). The baseline image was recorded prior to acid addition. In another set of experiments, MBs were added to prewarmed PBS with preadjusted pH. Starting from the baseline, the signal intensity was monitored until it reached a plateau. To assess reversibility, the MB signal was monitored as the pH was alternated by adding HCl or NaOH. All experiments were performed in triplicate, each using separate MB batches.

Image and Intensity Kinetic Analysis.

Images were captured at preset time points using IC capture (The ImagingSource, LLC). The intensities within ellipsoidal ROIs were calculated by ImageJ and are presented as the mean gray value (range from 0 to 256). Fold increase in signal intensity was calculated by dividing the signal at each time point by the signal at baseline. Time-intensity curves (TICs) to assess the rate of signal change at each pH were generated by capturing an image every 5 s, plotting the 20 s moving average of the ROI intensity, and fitting the data to asymmetric sigmoidal curves (Microsoft Excel; GraphPad Prism). The time to half-maximum of the fitted sigmoid curve was plotted against the carbon chain length (Figure 3B). Experiments were performed in triplicate by using independent batches of PC-MBs.

Microbubble Simulations.

CPS and B-mode signal changes of MBs in response to changes in elasticity were modeled by the Rayleigh Plesset Equation with extensions by the Marmottant. Ideal pulses at 7 and 1.5 MHz were used at a pressure of 185 kPa (similar to our estimated mechanical index during imaging studies). Additional details are provided in the Supporting Information.

RESULTS AND DISCUSSION

Variations of pH Affect Nonlinear Signal Intensity of PC-MBs.

To assess the effect of pH on the nonlinear signal intensity of PC-MBs, PFB-filled MBs were formulated with 10% 18:0 PE-PEG2k and 90% either 18:0 PC or 16:0 PC. When the pH of these MB suspensions was decreased, harmonic signal intensity increased and plateaued within minutes (Figure 2). Baseline-corrected harmonic signals for both the 18:0 and 16:0 PC-MBs showed a stark signal increase of ~35 AU as the pH decreased from 7.5

to ~5.5 (Figure 2A). This corresponds to a 3.0 and a 2.6-fold increase over the baseline (Figure S1). This was followed by a less pronounced increase between pH 5.5 and 2.7. Heterogeneity of the CPS signal intensity within the presented images is attributed to the position of the focal zone, which is positioned at the lower border of the imaging chamber.

Lumason MBs, which are FDA approved CEUS agents composed of a sulfur hexafluoride core stabilized by 16:0 PC and DPPG-Na (1,2-dipalmitoyl-*sn*-glycero-3-phospho-*rac*-glycerol sodium) lipids, behaved similarly but exhibited a lesser signal increase compared to our PC-MB formulations (Figure 2A,B). Note that in addition to differences in lipid and gas compositions, the average MB diameter of Lumason is smaller (1.6 μm vs 2.0 and 2.4 μm for the 18:0 and 16:0 PC-MBs, respectively) (Figure S2). Since smaller MBs exhibit higher interfacial tension (inversely proportional to the radius), it could in part explain the difference in signal at lower pH. Importantly, PFC gas and liquid are known to further lower the interfacial tension of bubbles as they intercalate with lipid membranes, producing a cosurfactant effect.[25] More recently, the correlation between improved MB stability and the lowered surface tension (and consequently, Laplace pressure) has been reported in PFB MBs containing perfluorohexane incorporated into the lipid shell.[26] Lumason, by comparison, contains a core of sulfur hexafluoride gas, which is not currently known to intercalate in lipid chains.

Taken together, these results demonstrate for the first time that PC-MBs are able to exhibit acoustic signal modulation in response to changes in pH, with the greatest change occurring within the physiologic range. This phenomenon likely occurs due to the self-assembly behavior of phospholipids and does not require the MBs shell to be reengineered. We have also demonstrated that this property is exhibited by Lumason. Definity, the other PC-MB approved clinical agent that was not evaluated in this study, will likely be pH sensitive since it has a composition similar to that of our own formulation. Importantly, while effective pH-sensitive ultrasound contrast media have been developed and reported previously, these exhibit increased backscatter in response to reduced pH rather than taking advantage of nonlinear oscillation.[27]

To ensure that the changes in harmonic signal are not due to transient and local HCl concentration, PC-MBs were added to PBS with preadjusted pH. The rates of signal intensity increase and plateau were similar. Although not physiologically relevant, increasing the pH to 8 and 11 caused only minimal to modest increases in the harmonic signal (Figure S3). Similar activation behavior was observed when imaging at 1.5 MHz as described above for 7.0 MHz (Figure S4). This suggests that the acid-mediated behavior of PC-MBs is due to inherent changes in MBs and is independent of the frequency. The lack of dependence of the pH-induced harmonic signal increase on frequency is clinically important, as lower frequencies are necessary for CEUS examination of deeper structures such as the liver, whereas higher frequencies are used for superficial structures such as lymph nodes. It is not expected that MBs will be directly exposed to the tumor interstitium when imaging solid tumors because MBs are blood pool agents. Excess protons diffuse along a concentration gradient from the acidic tumor microenvironment into the blood to be buffered and washed away. Nonetheless serum pH is expected to be lower than normal.[28,29] We anticipate that MBs traversing the abnormal larger intratumoral capillaries will increase

their residence time to be affected by pH. This effect could be further enhanced by targeting MBs to the tumor endothelium to increase the exposure time.

Lipid Structure of the MB Shell Modulates Acid-Induced Activation.

We noted a difference in acid-activation behavior between the 18:0 and 16:0 PC-MBs. 16:0 PC-MBs exhibited activation at a slightly higher pH, closer to 7.4, compared to 18:0 PC-MBs, which only showed activation below a pH of 7.0 (Figure 2A,B). By comparison, Lumason exhibited an increased signal when the pH decreased below 6.45. These differences were hypothesized to be due in part to differences in the chemical structures of the PC-MB shell lipids. To further evaluate the effect of acyl chain lengths on harmonic signal, TICs for acid-activation were generated for the 14:0, 16:0, 18:0, and 20:0 PC-MBs as the pH was adjusted from 7.4 to 6.4 and 3.0 (Figure 3A). Although the time to half-maximum was greater for MBs with the longer acyl-chain length lipids, their signal enhancement was greater compared to that of MBs with shorter acyl-chain length lipids (Figure 3B). This difference in signal amplitude is attributed in part to the differences in the initial signal intensity for these PC-MBs (Figure S5). Because of these stark differences in activation rates between PC-MBs with different acyl chain lengths, we hypothesized that the longer time to full activation of the longer chain length lipids was largely due to slower conformational changes caused by the stronger intermolecular forces between acyl chains.[30,31] Diffusion of hydronium ions throughout the solution is unlikely to limit the time of activation, as shorter acyl chain PCs demonstrated near instantaneous activation (14:0 PC and 16:0 PC vs 20:0 PC).

We also investigated the effect of removing the phosphate group from the lipid polar head on the acid-activation behavior of the MBs. PC is a neutral zwitterionic phospholipid comprised of a quaternary ammonium that is unable to accept a proton and a modified phosphate group. As the pK_a of the phosphate in PCs is approximately 1, PCs and PC monolayers have no net charge within the physiologic pH range.[32,33] MBs were prepared with 18:0 TAP, a cationic lipid that does not contain a phosphate group. These MBs exhibited no changes in harmonic signal intensity in response to a pH decrease of 3.0 (Figure 4). Taken together, these results suggest that despite the low pK_a of phosphate moieties in PCs, interaction of hydronium ions with the phosphate of PCs has an effect on MB oscillation.

In bilayer lipid membranes, and despite being neutral, PCs are known to exhibit changes in their molecular packing and mechanical properties with variations in pH, attributed to conformational changes in polar head packing and acyl chain orientation.[33,34] Owing to the fact that the interfacial tensions of curved micrometer-sized bubbles and flat surfaces are similar, the gas/water interface with intervening phospholipids can be simulated and studied using surface pressure–area per molecule isotherms and fluorescence microscopy.[35] Surface tension measurements carried out with a monolayer of PCs at the air–water interface using a Langmuir trough demonstrated that surface tension is dependent on the pH of the subphase. Specifically, the surface tension was at its minimum for pH values close to the PC isoelectric point (4.15),[36] resulting from the increased concentration of H^+ that induced a spontaneous close packing of polar heads due to ionic interactions. Interestingly, a higher lipid surface concentration at low pH has also been observed with the negatively charged phospholipid

1,1′,2,2′-tetramyristoyl cardiolipin (TMCL).[37] Surface pressure–molecular area isotherms of TMCL confirmed the pH-dependence of the lipid packing and conformation. The lower surface area occupied per lipid in their liquid condensed phase (88 $Å^2$ at pH 4 vs 91 $Å^2$ at pH 7) is in agreement with a higher packing of lipids before film collapse and higher surface concentration. Longer plateaus of coexistence between a liquid-expanded (LE) phase and liquid-condensed (LC) phase reveals a higher propensity of the lipophilic chains to adopt an ordered state at low pH, resulting in a concentration of the extended lipid at the surface. Both of these findings were attributed to changes in orientation of the polar head, leading to a maximal concentration of hydrophobic side chains extended at the surface. Interestingly, these domains of high lipid concentration domains are visible as condensed regions of saturated lipid in coexistence with the PEG-lipid expanded fluid phase on MBs observed by fluorescence microscopy combined with Langmuir trough experiments.[35] These microstructures were shown to influence MB lipid shell physical characteristics such as surface viscosity and shear yield and expected to affect gas permeability and lipid shedding.[35]

Importantly, kinetic modeling indicates that when lipid-coated MBs oscillate at low driving pressure, they exhibit elastic behavior, whereas at higher driving pressures, they undergo surface tension changes that can reach that of water upon expansion/rupture, and surface tension decreases to zero when the lipid shell buckles.[8,38] These asymmetric changes in surface tension result in nonlinear oscillation of MBs that occurs within the expected pressure range of a clinical ultrasound scanner. Taken together with prior findings of pH-dependence of the surface tension of lipid films, we hypothesize that the interactions of PCs on the MB surface with hydronium ions in solution result in a more cohesive lipid monolayer and greater propensity of the PCs in the shell to resist fracture during lipid shedding and reformation during fragmentation. We also hypothesize that this phenomenon is associated with changes in shell elasticity. Note that this hypothetical explanation of the pH-driven increase in stability against acoustic dissolution and overall higher echogenicity is also in agreement with theoretical simulations.

In order to better understand the proposed causes for this phenomenon, we simulated MB responses to changes in shell elasticity using the Rayleigh–Plesset equation with Marmottant extensions.[38,39] Idealized pulses with a peak negative pressure of 185 kPa and frequencies of both 1.5 and 7 MHz (similar to our mechanical indices and center frequency for ultrasound experiments) were used. With increases in the independent parameter of elasticity, the intensity of the CPS echoes increased by up to 3-fold, consistent with experimental results. This was true for both simulated center frequencies. However, smaller diameter MBs had a greater increase in the CPS echo at 1.5 MHz, and higher diameter MBs had a greater increase in the CPS echo at 7 MHz. The relative magnitude of the response, with respect to the response as soft elasticity (X = 0.5 N/m), is shown in Figure 5. The spectral content of frequencies higher than the pulsing center frequency, including harmonics, increased for both center frequencies and all MB diameters (Figure S6). Representative waveforms of the B-mode and CPS pressure echoes are depicted in Figure S7. As there are many shell parameters for this new formulation of PC-MBs (e.g., elasticity, viscosity, and surface tension) that have not yet been determined, shell elasticity changes driven by pH change are a possible explanation for the measured intensity changes.

Acid-Induced Activation of PC-MBs is Reversible.

For both 18:0 and 16:0 PC-MBs, we were able to reverse the acid-induced activation to the baseline by adding NaOH to normalize the pH back to 7.4. These cycles were repeated three times after waiting over 8 min to ensure that both maximum and minimum harmonic signals were reached. While the MB signal returned to nearly the same baseline value, there was an observable decrease in maximal signal with each cycle, likely due to MB destruction (Figure 6). Lumason and non-PEGylated 18:0 PC-MBs also showed similar reversibility, suggesting that this phenomenon occurs independently of the presence of PEG (Figure S8). When tested at lower frequencies to mimic the clinical frequencies used in abdominal imaging, both Lumason and PC-MBs showed reversible activation when imaged with the 4 V1 transducer transmitting at 1.5 MHz (Figure S9). Notably, the B-mode signal also exhibited a modest increase in signal with each activation cycle, suggesting that pH may impact MB backscatter (Figure S10). The near complete reversibility of this phenomenon when the ambient pH is alternated between an acidic to a basic state further supports the hypothesis that the effect observed is due to conformational changes of the PC monolayer rather than degradation.

CONCLUSION

Our work demonstrates for the first time the intrinsic pH-sensitive characteristics of PC-MBs that result in quantifiable changes in nonlinear oscillation. PC-MBs exhibit a marked increase in harmonic signal intensity (observable using a clinical ultrasound scanner) with a reduction in pH from 7.5 to 5.5. Furthermore, this phenomenon is dependent on the chemical properties of the MB shell, specifically the length of acyl chains and the presence of phosphate in the polar head. Regional acidosis in deep tissues can occur under certain pathophysiologic states (e.g., solid tumors), raising the possibility that enhancement of these tissues in CEUS exams may in part be due to pH changes, in addition to blood flow, fractional blood volume, and MB concentration.

Supplementary Material

Refer to Web version on PubMed Central for supplementary material.

ACKNOWLEDGMENTS

The authors would like to thank David Fetzer, MD, for his intellectual contribution in experimental design and data interpretation. The authors would like to acknowledge Siemens Medical Solutions USA, Inc., for loaning them the ultrasound equipment, and for the implementation of the MRSQ software on the ultrasound scanner. This work was funded by the RSNA Resident Research Grant RR2102, awarded to SA. SA is a NIH T32 trainee (1T32EB028093). This work was also supported in part by the Cancer Prevention and Research Institute of Texas (CPRIT) Grant RR150010. RFM is a CPRIT Established Investigator.

ABBREVIATIONS

CEUS	Contrast-enhanced ultrasound
PC	Phosphatidylcholine
MB	Microbubble

PEG	Polyethylene glycol
CPS	Cadence contrast pulse sequencing
TIC	time-intensity curve

REFERENCES

(1). Yusefi H; Helfield B Ultrasound Contrast Imaging: Fundamentals and Emerging Technology. Front Phys 2022.

(2). Whittingham TA; Whittingham TA Contrast-Specific Imaging Techniques: Technical Perspective. Contrast Media in Ultrasonography 2005, 43–70.

(3). Quaia E Assessment of Tissue Perfusion by Contrast-Enhanced Ultrasound. Eur. Radiol 2011, 21 (3), 604–615. [PubMed: 20927527]

(4). Lee H; Kim H; Han H; Lee M; Lee S; Yoo H; Chang JH; Kim H Microbubbles Used for Contrast Enhanced Ultrasound and Theragnosis: A Review of Principles to Applications. Biomed Eng. Lett 2017, 7 (2), 59–69. [PubMed: 30603152]

(5). Schutt EG; Klein DH; Mattrey RM; Riess JG Injectable Microbubbles as Contrast Agents for Diagnostic Ultrasound Imaging: The Key Role of Perfluorochemicals. Angew. Chem., Int. Ed. Engl 2003, 42 (28), 3218–3235. [PubMed: 12876730]

(6). Ferrara K; Pollard R; Borden M Ultrasound Microbubble Contrast Agents: Fundamentals and Application to Gene and Drug Delivery. Annu. Rev. Biomed Eng 2007, 9, 415–447. [PubMed: 17651012]

(7). Sojahrood AJ; Haghi H; Karshafian R; Kolios MC Nonlinear Dynamics and Bifurcation Structure of Ultrasonically Excited Lipid Coated Microbubbles. Ultrason Sonochem 2021, 72, 105405. [PubMed: 33360533]

(8). Versluis M; Stride E; Lajoinie G; Dollet B; Segers T Ultrasound Contrast Agent Modeling: A Review. Ultrasound Med. Biol 2020, 46 (9), 2117–2144. [PubMed: 32546411]

(9). Leong-Poi H; Song J; Rim SJ; Christiansen J; Kaul S; Lindner JR Influence of Microbubble Shell Properties on Ultrasound Signal: Implications for Low-Power Perfusion Imaging. Journal of the American Society of Echocardiography 2002, 15, 1269–1276. [PubMed: 12411916]

(10). Sojahrood AJ; Yang C; Counil C; Nittachayarn P; Goertz DE; Exner AA; Kolios MC Shell Elasticity and Viscosity of Lipid-Coated Microbubbles Are Significantly Altered in Mediums of Different Ionic Strength. arXiv, 2023, DOI: 10.48550/arXiv.2307.13827.

(11). Li Q; Matula TJ; Tu J; Guo X; Zhang D Modeling Complicated Rheological Behaviors in Encapsulating Shells of Lipid-Coated Microbubbles Accounting for Nonlinear Changes of Both Shell Viscosity and Elasticity. Phys. Med. Biol 2013, 58 (4), 985–998. [PubMed: 23339902]

(12). Qin D; Lei S; Wang X; Zhong X; Ji X; Li Z Resonance Behaviors of Encapsulated Microbubbles Oscillating Nonlinearly with Ultrasonic Excitation. Ultrason Sonochem 2023, 94, No. 106334.

(13). Dubey D; Christiansen MG; Vizovisek M; Gebhardt S; Feike J; Schuerle S Engineering Responsive Ultrasound Contrast Agents Through Crosslinked Networks on Lipid-Shelled Microbubbles. Small 2022, 18 (12), 2107143.

(14). Nakatsuka MA; Mattrey RF; Esener SC; Cha JN; Goodwin AP Aptamer-Crosslinked Microbubbles: Smart Contrast Agents for Thrombin-Activated Ultrasound Imaging. Adv. Mater 2012, 24 (45), 6010–6016. [PubMed: 22941789]

(15). Lux J; Vezeridis AM; Hoyt K; Adams SR; Armstrong AM; Sirsi SR; Mattrey RF Thrombin-Activatable Microbubbles as Potential Ultrasound Contrast Agents for the Detection of Acute Thrombosis. ACS Appl. Mater. Interfaces 2017, 9 (43), 37587–37596. [PubMed: 28994575]

(16). Borden MA; Kruse DE; Caskey CF; Zhao S; Dayton PA; Ferrara KW Influence of Lipid Shell Physicochemical Properties on Ultrasound-Induced Microbubble Destruction. IEEE Trans Ultrason Ferroelectr Freq Control 2005, 52 (11), 1992–2002. [PubMed: 16422411]

(17). Pérez-Tomás R; Pérez-Guillén I Lactate in the Tumor Microenvironment: An Essential Molecule in Cancer Progression and Treatment. Cancers (Basel) 2020, 12 (11), 3244. [PubMed: 33153193]

(18). Fischer K; Hoffmann P; Voelkl S; Meidenbauer N; Ammer J; Edinger M; Gottfried E; Schwarz S; Rothe G; Hoves S; Renner K; Timischl B; Mackensen A; Kunz-Schughart L; Andreesen R; Krause SW; Kreutz M Inhibitory Effect of Tumor Cell-Derived Lactic Acid on Human T Cells. Blood 2007, 109 (9), 3812–3819. [PubMed: 17255361]

(19). Webb BA; Chimenti M; Jacobson MP; Barber DL Dysregulated PH: A Perfect Storm for Cancer Progression. Nat. Rev. Cancer 2011, 11 (9), 671–677. [PubMed: 21833026]

(20). Pillai SR; Damaghi M; Marunaka Y; Spugnini EP; Fais S; Gillies RJ Causes, Consequences, and Therapy of Tumors Acidosis. Cancer Metastasis Rev 2019, 38 (1–2), 205–222. [PubMed: 30911978]

(21). Anemone A; Consolino L; Arena F; Capozza M; Longo DL Imaging Tumor Acidosis: A Survey of the Available Techniques for Mapping in Vivo Tumor PH. Cancer Metastasis Rev 2019, 38 (1–2), 25–49. [PubMed: 30762162]

(22). Anemone A; Consolino L; Conti L; Irrera P; Hsu MY; Villano D; Dastrú W; Porporato PE; Cavallo F; Longo DL Tumour Acidosis Evaluated in Vivo by MRI-CEST PH Imaging Reveals Breast Cancer Metastatic Potential. British Journal of Cancer 2020 124:1 2021, 124 (1), 207–216.

(23). Brambila CJ; Lux J; Mattrey RF; Boyd D; Borden MA; De Gracia Lux C Bubble Inflation Using Phase-Change Perfluorocarbon Nanodroplets as a Strategy for Enhanced Ultrasound Imaging and Therapy. Langmuir 2020, 36 (11), 2954–2965. [PubMed: 32090572]

(24). De Gracia Lux C; Vezeridis AM; Lux J; Armstrong AM; Sirsi SR; Hoyt K; Mattrey RF Novel Method for the Formation of Monodisperse Superheated Perfluorocarbon Nanodroplets as Activatable Ultrasound Contrast Agents. RSC Adv 2017, 7 (77), 48561–48568. [PubMed: 29430294]

(25). Szíjjártó C; Rossi S; Waton G; Krafft MP Effects of Perfluorocarbon Gases on the Size and Stability Characteristics of Phospholipid-Coated Microbubbles: Osmotic Effect versus Interfacial Film Stabilization. Langmuir 2012, 28 (2), 1182–1189. [PubMed: 22176688]

(26). Abou-Saleh RH; Peyman SA; Johnson BRG; Marston G; Ingram N; Bushby R; Coletta PL; Markham AF; Evans SD The Influence of Intercalating Perfluorohexane into Lipid Shells on Nano and Microbubble Stability. Soft Matter 2016, 12 (34), 7223–7230. [PubMed: 27501364]

(27). Walker JA-T; Wang X; Peter K; Kempe K; Corrie SR Dynamic Solid-State Ultrasound Contrast Agent for Monitoring PH Fluctuations In Vivo. ACS Sens 2020, 5 (4), 1190–1197. [PubMed: 32202414]

(28). Martin NK; Gaffney EA; Gatenby RA; Gillies RJ; Robey IF; Maini PK A Mathematical Model of Tumour and Blood PHe Regulation: The [··· Formula···] Buffering System. Math Biosci 2011, 230 (1), 1. [PubMed: 21167185]

(29). Zhang X; Lin Y; Gillies RJ Tumor PH and Its Measurement. J. Nucl. Med 2010, 51 (8), 1167–1170. [PubMed: 20660380]

(30). Lee S; Kim DH; Needham D Equilibrium and Dynamic Interfacial Tension Measurements at Microscopic Interfaces Using a Micropipet Technique. 2. Dynamics of Phospholipid Monolayer Formation and Equilibrium Tensions at the Water–Air Interface. Langmuir 2001, 17 (18), 5544–5550.

(31). Borden MA Intermolecular Forces Model for Lipid Microbubble Shells. Langmuir 2019, 35 (31), 10042–10051. [PubMed: 30543753]

(32). Moncelli MR; Becucci L; Guidelli R The Intrinsic PKa Values for Phosphatidylcholine, Phosphatidylethanolamine, and Phosphatidylserine in Monolayers Deposited on Mercury Electrodes. Biophys. J 1994, 66 (6), 1969–1980. [PubMed: 8075331]

(33). Akimov SA; Polynkin MA; Jiménez-Munguía I; Pavlov KV; Batishchev OV Phosphatidylcholine Membrane Fusion Is PH-Dependent. Int. J. Mol. Sci 2018, 19 (5), 1358. [PubMed: 29751591]

(34). Zhou Y; Raphael RM Solution PH Alters Mechanical and Electrical Properties of Phosphatidylcholine Membranes: Relation between Interfacial Electrostatics, Intramembrane Potential, and Bending Elasticity. Biophys. J 2007, 92 (7), 2451–2462. [PubMed: 17172308]

(35). Borden MA; Pu G; Runner GJ; Longo ML Surface Phase Behavior and Microstructure of Lipid/PEG-Emulsifier Monolayer-Coated Microbubbles. Colloids Surf. B Biointerfaces 2004, 35 (3–4), 209–223. [PubMed: 15261034]

(36). Brzozowska I; Figaszewski ZA The Influence of PH on Phosphatidylcholine Monolayer at the Air/Aqueous Solution Interface. Colloids Surf. B Biointerfaces 2003, 27 (4), 303–309.

(37). Sturm M; Gutowski O; Brezesinski G The Effect of PH on the Structure and Lateral Organization of Cardiolipin in Langmuir Monolayers. ChemPhysChem 2022, 23 (19), e202200218. [PubMed: 35920819]

(38). Marmottant P; van der Meer S; Emmer M; Versluis M; de Jong N; Hilgenfeldt S; Lohse D A Model for Large Amplitude Oscillations of Coated Bubbles Accounting for Buckling and Rupture. J. Acoust Soc. Am 2005, 118 (6), 3499–3505.

(39). Brown KG; Hoyt K Evaluation of Nonlinear Contrast Pulse Sequencing for Use in Super-Resolution Ultrasound Imaging. IEEE Trans Ultrason Ferroelectr Freq Control 2021, 68 (11), 3347–3361. [PubMed: 34181537]

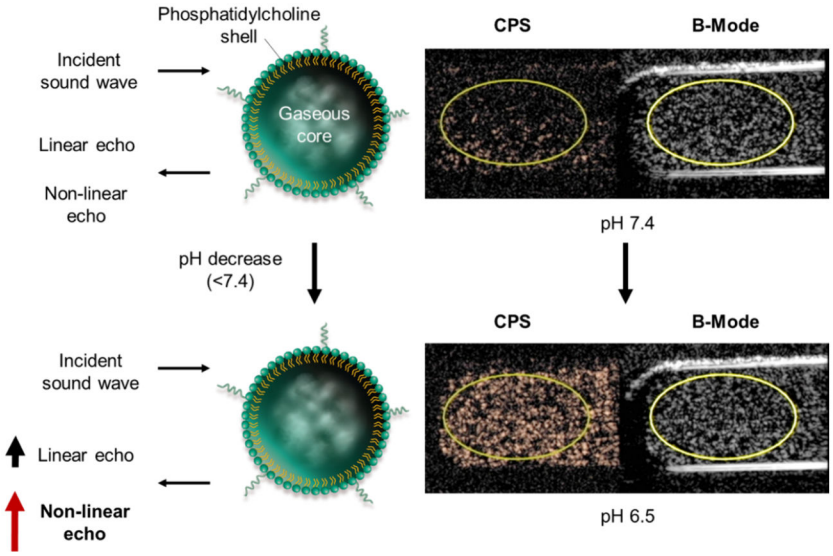

Figure 1.

Phosphatidylcholine-shell microbubbles (PC-MBs) are activated at acidic pH. Decrease of pH below a normal physiological level results in an increase in nonlinear echoes of PC-MBs (CPS: Cadence contrast Pulse Sequence).

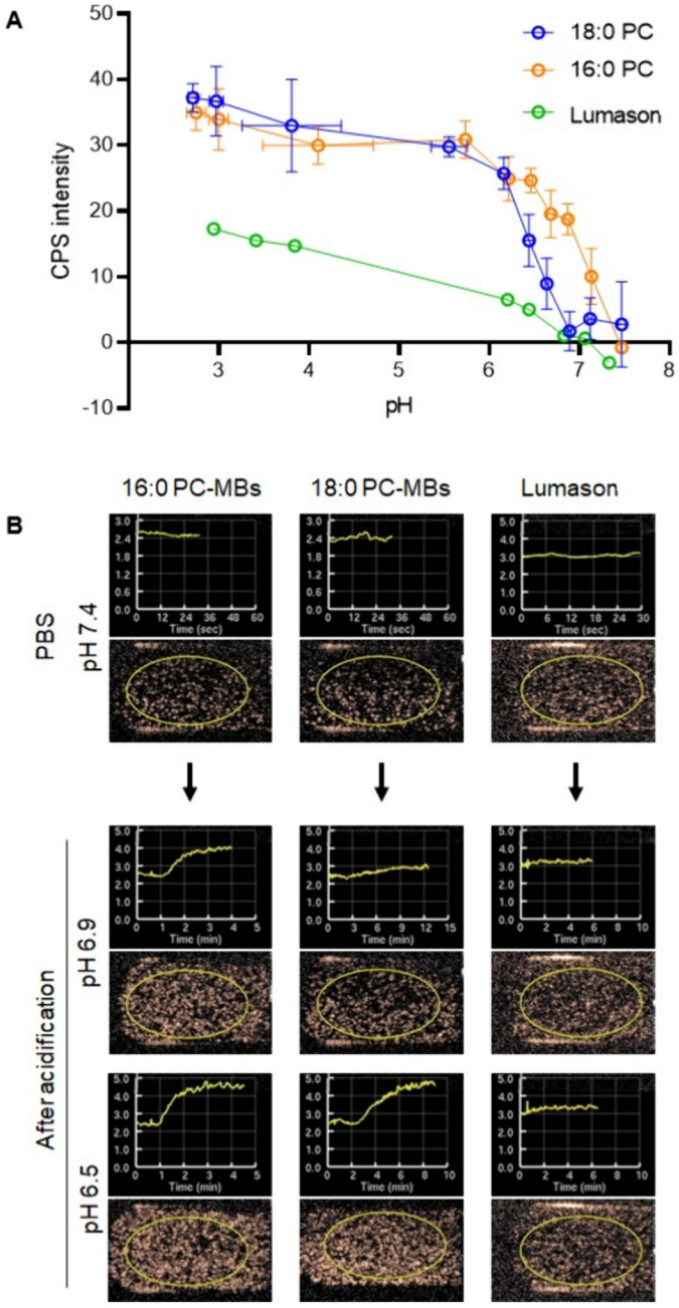

Figure 2.

Nonlinear signal intensity of PC-MBs is pH dependent. (A) Sharp increase in the CPS signal intensity of 16:0 and 18:0 PC-MBs is observed as pH decreases from 7.5 to 5.7 (error bars indicate SD; $n = 3$). The change in the signal of Lumason is far less pronounced. (B) Representative images acquired at the plateau following the acidification of the suspension. Note that there is a visible difference in the signals of the 16:0 and 18:0 PC-MBs and Lumason. Insets above each CPS image indicate time intensity curves for highlighted regions of interest.

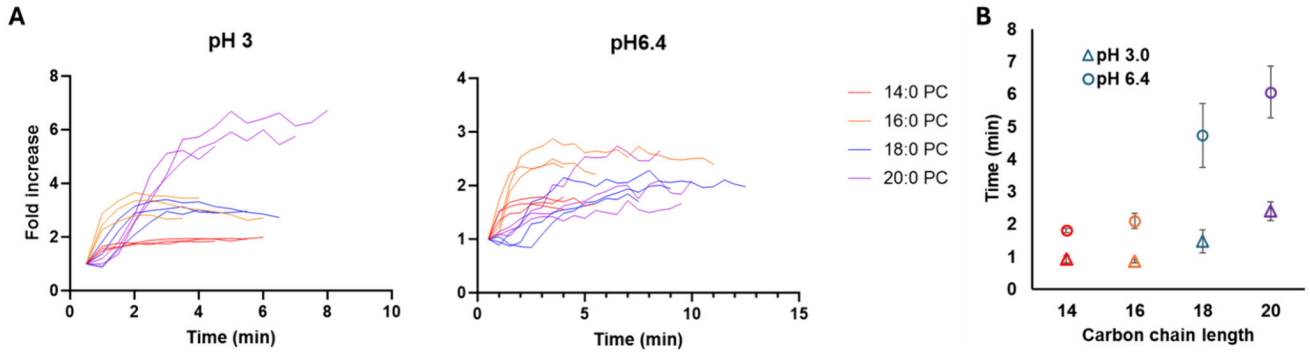

Figure 3.

Acid-activation kinetics of PC-MBs are dependent on MBs' shell lipid structure. (A) Fold-increase in signal intensity of PC-MBs containing 14:0, 16:0, 18:0, and 20:0 PCs demonstrates that shorter carbon chain lengths allow for faster activation. (B) Mean time to half-maximum ± SD of the time-dependent signals shown in (A) fitted to asymmetric sigmoid functions. Time to half-maximum increases for longer carbon chain lengths at both pH levels tested.

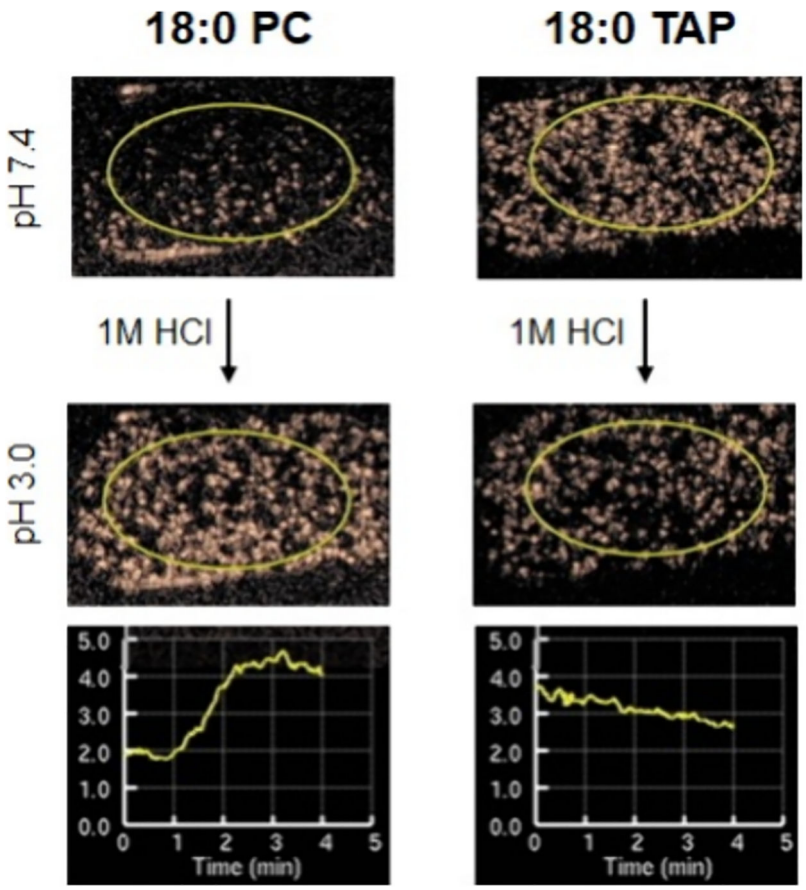

Figure 4.

Acid-activation of MBs requires phosphate. MBs composed of 18:0 TAP had no appreciable increase in harmonic signal upon acidification.

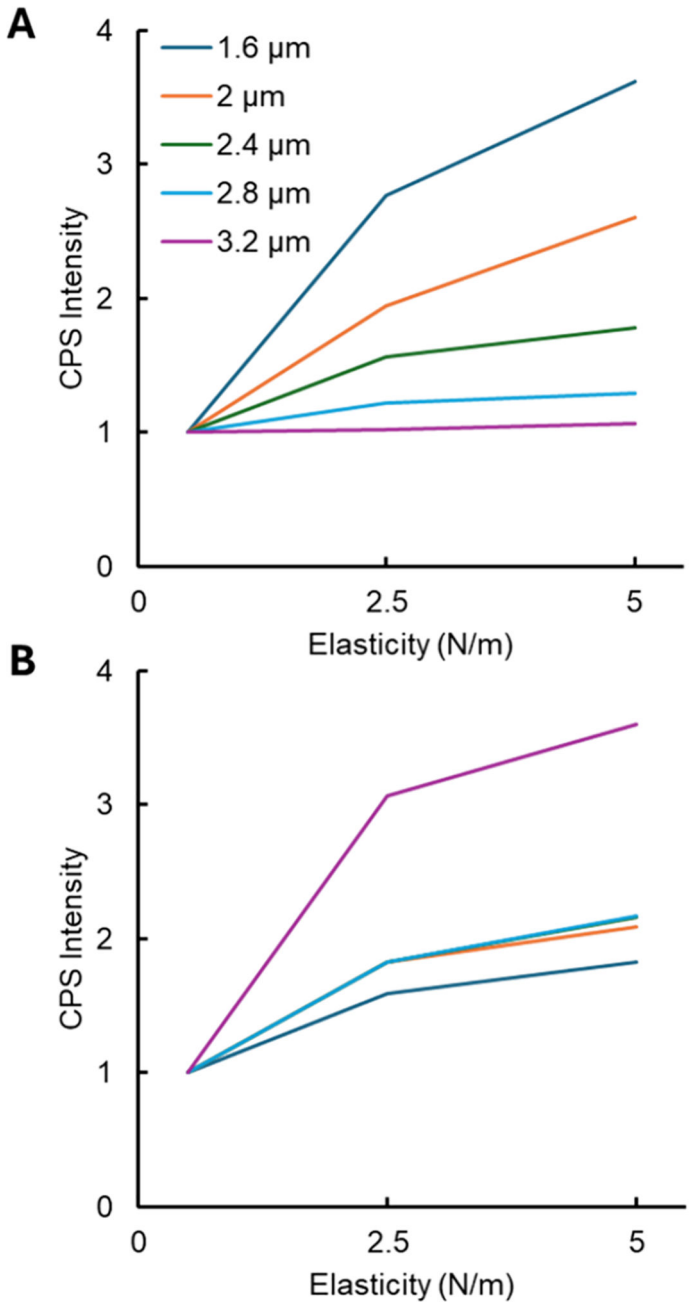

Figure 5.
Simulated MBs demonstrate increased CPS intensity with increased elasticity. Simulated MB responses to pulses of 1.5 MHz (A) and 7 MHz (B) show that CPS intensity is dependent on both elasticity and MB diameter.

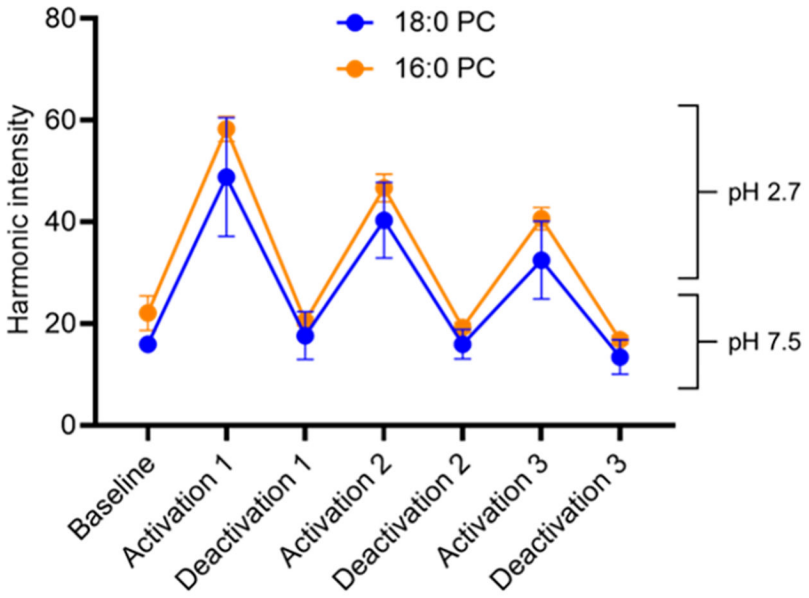

Figure 6.

Acid-activation of PC-MBs is reversible. Repeated cycles of pH-dependent activation and deactivation demonstrate marked increases in CPS signal intensity for PC-MBs (16:0 PC and 18:0 PC) compared to the baseline. Decreased CPS signal intensity upon repeated cycles is attributed to microbubble destruction.